


Hypermethylation-Mediated lncRNA MAGI2-AS3 Downregulation Facilitates Malignant Progression of Laryngeal Squamous Cell Carcinoma via Interacting With SPT6

Cell Transplantation
Volume 32: 1–18
© The Author(s) 2023
Article reuse guidelines:
sagepub.com/journals-permissions
DOI: 10.1177/09636897231154574
journals.sagepub.com/home/cll


Jiantao Wang¹, Chuan Yang¹, Huan Cao¹, Jianwang Yang¹,
Wenxia Meng¹, Miaomiao Yu¹, Lei Yu¹, and Baoshan Wang¹ 

Abstract

Long noncoding RNAs (lncRNAs) have an effect on the occurrence and progression of a considerable number of diseases, especially cancer. Existing research has suggested that MAGI2 antisense RNA 3 (MAGI2-AS3) takes on a critical significance in the development of hepatocellular carcinoma and lung cancer. However, the functions of MAGI2-AS3 in laryngeal squamous cell carcinoma (LSCC) remain unclear. In this study, MAGI2-AS3 expression level in LSCC tissue and cell lines was detected, and the effect of MAGI2-AS3 overexpressed on LSCC phenotypes and the possible influence mechanisms were examined. MAGI2-AS3 was downregulated in the tissues of LSCC patients versus non-tumor tissues, and it was correlated with advanced TNM (tumor, node, metastasis) stage and lymph node metastases, as indicated by the results of this study. MAGI2-AS3 inhibited the proliferation, migration, and invasion of LSCC cells *in vitro* and *in vivo*. Furthermore, the hypermethylation level of the MAGI2-AS3 promoter region was indicated by bisulfite genomic sequencing and methylation-specific polymerase chain reaction, such that MAGI2-AS3 expression was downregulated. Besides, MAGI2-AS3 promoter hypermethylation was regulated by DNA methyltransferase 1 (DNMT1), and MAGI2-AS3 expression was reversed by 5-Aza-2'-deoxycytidine (5-Aza). Moreover, the result of the RNA pull-down experiment suggested that 38 proteins were enriched in the MAGI2-AS3 group versus the control group in TUI77 cells. To be specific, SPT6 (ie, a conserved protein) was enriched by fold change >10. SPT6 knockdown reduced the antitumor effect of MAGI2-AS3 in TUI77 and AMC-HN-8 cells. Meanwhile, SPT6 overexpression inhibited the proliferation, metastasis, and invasion of TUI77 and AMC-HN-8 cells. As revealed by the above findings, DNMT1-regulated MAGI2-AS3 promoter hypermethylation led to downregulated MAGI2-AS3 expression, such that the presence and progression of LSCC were inhibited in an SPT6 binding-dependent manner.

Keywords

laryngeal squamous cell carcinoma, MAGI2-AS3, DNA methylation, SPT6, biomarker

Introduction

Laryngeal squamous cell carcinoma (LSCC) takes up nearly 90% of all laryngeal malignancies and has the second highest incidence among all types of head and neck squamous cell carcinoma (HNSCC)^{1,2}. The methods for the treatment of LSCC comprise surgery, radiotherapy, chemotherapy, and immunotherapy. To be specific, surgery has still been the primary treatment method. However, some problems after surgical treatment (eg, recurrence, metastasis, and chemoresistance) should be addressed to improve their prognosis. As molecular diagnostic technology has been leaping forward, numerous tumor markers have been detected and identified in lung cancer, breast cancer, and so forth, and the corresponding

molecular-targeted drugs supply a type of effective measure for tumor treatment. Thus, it is of great clinical significance to explore new target molecules of LSCC for its treatment.

¹ Department of Otorhinolaryngology, The Second Hospital of Hebei Medical University, Shijiazhuang, China

Submitted: January 24, 2022. Revised: January 12, 2023. Accepted: January 16, 2023.

Corresponding Author:

Baoshan Wang, Department of Otorhinolaryngology, The Second Hospital of Hebei Medical University, 215 Heping West Road, Shijiazhuang 050000, China.
Email: hebwangbs@163.com



Long noncoding RNAs (lncRNAs) are defined as RNA transcripts greater than 200 nucleotides in length without the protein-coding potential. Mechanism investigations have revealed that antisense lncRNAs are capable of affecting the biological processes in the cytoplasm and nucleus. lncRNAs in the cytoplasm inhibit microRNAs (miRNAs) in the mechanism of competing endogenous RNAs (ceRNAs)³, while those in the nucleus play a role in translational control and epigenetic modulations. However, lncRNAs can be transported from the nucleus to the plasma in several cases⁴. As sequencing technology and other clinical techniques are advancing, emerging evidence has suggested that lncRNAs are vital regulatory factors in cellular development and human diseases (eg, cancer). Dysregulation of lncRNAs has been identified in almost all types of cancer, and they serve as tumor promoters or suppressors⁵. Moreover, well-documented examples have suggested that lncRNAs have putative oncogenic or tumor suppressor activity across a wide variety of tumors (eg, hepatocellular carcinoma, esophageal cancer, and breast cancer)⁴. However, the research on lncRNAs in LSCC has been rare and remains at the preliminary stage.

Moreover, some differentially expressed lncRNAs were identified in some cancers, and potential functions were revealed. For instance, overexpression of lncRNA FGD5-AS1 enhanced cisplatin resistance through the miR-497-5p/SEPT2 axis in LSCC⁶. lncRNA ZNF667-AS1 was downregulated by methylation and served as tumor suppressor genes in LSCC⁷. Furthermore, LINC00319 and lncRNA DLEU2 enhanced the malignant properties in LSCC^{8,9}. Nevertheless, more differentially expressed functional lncRNAs should be identified to successfully provide reliable targets for LSCC treatment.

Existing research has suggested that epigenetics takes on a critical significance to LSCC development and progression¹⁰. DNA methylation refers to one of the most characteristic epigenetic modifications, and it is capable of regulating gene transcription. Accordingly, changes in DNA methylation patterns play a certain role in the genesis and development of tumors. Abnormal genome-wide DNA methylation has been identified early in tumor development of some types of cancer (eg, esophageal cancer and lung cancer), which affects gene stability and facilitates cellular transformation. There is a considerable amount of evidence that lncRNAs are correlated with the regulation of DNA methylation. DNA hypermethylation that often causes transcriptional silencing serves as a vital tumor suppressor¹¹. Yang et al.¹² have suggested that the downregulated expression of lncRNA ZNF582-AS1 due to DNA hypermethylation facilitated clear cell renal cell carcinoma growth. Moreover, Wang et al.¹³ have suggested that aberrant methylation-mediated downregulation of lncRNA SSTR5-AS1 promoted LSCC progression and metastasis. However, the specific clinical significance of lncRNAs in LSCC and its DNA methylation status, and the molecular mechanism remain unclear.

lncRNAs affect tumor cells in a variety of ways, including miRNA sponges, RNA-binding protein scaffolds, transcription regulators, protein translation templates, and intermediates in RNA alternative splicing (AS). The most reported mechanism is that lncRNAs can serve as ceRNAs to relieve the suppression of miRNAs on the targeted gene expression¹⁴. Alternatively, lncRNAs are capable of exerting biological function through interaction with RNA-binding proteins (RBPs)¹⁵. For instance, LINC00162 can inhibit PTTG1IP expression by interacting with THRAP3, thus facilitating the proliferation of bladder cancer cell¹⁶.

Suppressor of Ty 6 Homolog (SPT6) is a conserved protein, which can directly interact with RNA polymerase II (RNAPII), histones, and the essential factor Iwsl. Recently, SPT6 has been reported to interact with the nuclear receptor binding SET domain protein 2 (NSD2) to facilitate interferon-induced transcription^{17,18}. SPT6 has been reported in breast cancer, colon cancer, and so on. For instance, Diao et al.¹⁹ have indicated that SPT6 promoted the proliferation and metastasis of colon cancer cells, whereas SPT6 knockdown induced apoptosis, stemness arrest, and chemosensitivity of these cancer cells.

In this study, the lncRNA microarray of LSCC tissues identified MAGI2 antisense RNA 3 (MAGI2-AS3) as one of the differentially expressed lncRNAs with high fold change and basal expression. The cohort study of LSCC patients further confirmed the downregulation of MAGI2-AS3 in LSCC tissues versus normal tissues and the correlation between downregulated MAGI2-AS3 expression, advanced TNM (tumor, node, metastasis) stage, and lymph node metastasis. Moreover, downregulated MAGI2-AS3 expression facilitated cell proliferation, migration, and invasion in combination with the regulation of epithelial–mesenchymal transition (EMT)-associated marker in TU177, AMC-HN-8 cell lines, and BALB/c nude mice. Besides, DNMT1-regulated DNA hypermethylation of gene promoter was proven to lead to the downregulation of MAGI2-AS3 in TU177 and AMC-HN-8 cells. In addition, MAGI2-AS3 could bind to SPT6, a transcription-related protein in TU177 cells, as indicated by the result of the RNA pull-down and RNA immunoprecipitation experiment. Moreover, SPT6 significantly inhibited the proliferation, migration, and invasion of TU177 and AMC-HN-8 cells, and the tumor-inhibiting effect of MAGI2-AS3 was SPT6-dependent.

Materials and Methods

Clinical Specimens

Sixty-one pairs of LSCC tumor tissues and matched normal tissues were acquired from patients with LSCC who underwent operation (Institute of Otolaryngology, Head and Neck Surgery of Hebei Medical University, Shijiazhuang, China). None of the patients had undergone any radiotherapy or chemotherapy before surgery. After surgery, the samples were

diagnosed based on pathology and quickly placed in liquid nitrogen until use. LSCC patients were classified in accordance with the TNM staging system of the Union for International Cancer Control (UICC). The study protocol conformed to the ethical review of research at the Second Hospital of Hebei Medical University. The informed consent of patients was signed before clinical specimens were acquired.

Cell lines, Culture, Treatment, and Cell Transfection

Human LSCC cell lines (TU177, AMC-HN-8) were cultured in the appropriate medium containing 10% fetal bovine serum (FBS; Sigma, NY, USA) and incubated in an incubator at 37°C with 5% CO₂ in a humidified atmosphere. TU177 cells were cultured in RPMI-1640 medium (Gibco, Grand Island, NY, USA), and AMC-HN-8 and 293T cells were maintained in Dulbecco's Modified Eagle Medium (DMEM; Gibco). TU177 and AMC-HN-8 cells were administrated with 7.5 μmol/l of 5-Aza-dC (Solarbio, Beijing, China) for 72 h. The sequence of MAGI2-AS3 was synthesized and then subcloned into the pcDNA3.1 plasmid to overexpress MAGI2-AS3 (Shenggong, Shanghai, China). Using Lipofectamine®2000 reagent (Invitrogen, Carlsbad, CA, USA) in accordance with the manufacturer's instruction, TU177 and AMC-HN-8 cells were transfected with the MAGI2-AS3 expression plasmid (oe-MAGI2-AS3) or the empty vector (oe-NC) as the control. The cells were harvested after 48 h of transfection for DNA and RNA extraction. The transfection efficiency was obtained through quantitative polymerase chain reaction (qPCR).

Microarray Analysis

Total RNA of four pairs of LSCC tissues and matched non-tumor tissues was extracted using the TRIzol reagent (Vazyme, Nanjing, China). The sample preparation and microarray hybridization were performed in accordance with Arraystar's standard protocols (Sangon Biotech, Shanghai, China).

Cell Proliferation, Transwell, Wound Healing, and Colony Formation Assays

The migration or invasion assays were performed using transwell inserts (Corning Incorporated, Corning, NY, USA) with and without Matrigel (BD Biosciences, Franklin Lakes, NJ, USA) coating, respectively. The transfected cells suspended in serum-free medium were seeded into the transwell inserts, and 10% FBS medium was placed at the bottom. After being cultured for 24 h, the cells were fixed with 4% paraformaldehyde solution (SEVEN, Beijing, China) and then dyed with 0.1% crystal violet (Solarbio). Subsequently,

the images were captured under a microscope at a magnification of 200×, and the number of cells penetrating the pores was obtained.

For the wound-healing assay, cells of 70%–80% density were plated in a six-well culture dish, and the cell monolayer was subsequently scratched with a 200-μl pipette tip. Representative images of cell migration were obtained at 0 and 48 h after injury. Remodeling was examined as the diminishing distance across the induced injury area normalized to the 0 h control and expressed as a relative migration rate.

Cell proliferation was assessed through the MTS assay (Promega, Madison, WI, USA). For this, 2×10^3 transfected cells were seeded in 96-well culture dishes with 100 μl of 10% serum medium per well. The 20-μl MTS solution was added per well every 24 h. Next, all plates were incubated for 2 h. The optical density (OD) was then examined by recording absorbance at 490 nm using Spark® multimode microplate reader (Mod: SPARK 10M; TECAN, Männedorf, Switzerland).

Cells transfected similarly were cultured in the respective plate of a six-well culture dish for the colony formation assay. The medium containing 10% FBS was changed every 5 days. After the medium was incubated for 12–14 days, the colonies were fixed with 4% paraformaldehyde and then dyed with 0.1% crystal violet by counting the number of dye that was adopted to examine the colony formation rate. All experiments were performed three times independently.

Western Blotting

The cells were harvested with radioimmunoprecipitation assay (RIPA) lysis buffer (Solarbio) containing phenylmethanesulfonyl fluoride (PMSF; Solarbio) and protease inhibitor cocktail (Solarbio). The lysates were removed through centrifugation at $12,000 \times g$ for 15 min at 4°C. The cell protein lysates were quantified, separated through sodium dodecyl sulfate-polyacrylamide gel electrophoresis, transferred onto a nitrocellulose membrane, and then blocked with 5% skim milk (BD Biosciences) prepared in $1 \times$ TBST with 0.05% Tween-20 (Solarbio). Subsequently, the membrane was incubated with specific primary antibodies, washed, and probed with horseradish-peroxidase-conjugated secondary antibody. Several antibodies such as E-cadherin (1:2,000 dilution, rabbit anti-human polyclonal antibody, #20874-1-AP; Proteintech, Wuhan, China), N-cadherin (1:6,000 dilution, rabbit anti-human polyclonal antibody, #22018-1-AP; Proteintech), Vimentin (1:2,000 dilution, rabbit anti-human polyclonal antibody, #10366-1-AP; Proteintech), and GAPDH (1:6,000 dilution, rabbit anti-human polyclonal antibody, #10494-1-AP; Proteintech) were used. Furthermore, the signals were detected using Molecular Imager® (Tanon, Shanghai, China).

MS2-12X-Dependent RNA Pull-Down Assay and Mass Spectrometry

The MS2-12X-dependent RNA pull-down experiments were performed using a Magna RNA-binding protein immunoprecipitation kit (Genesee Biotech, Guangzhou, China) in accordance with the manufacturer's instructions. TU177 cells were transfected with oe-MAGI2-AS3 and pcDNA3.1 plasmid for 48 h and then harvested. The cell lysates were incubated with buffer containing magnetic beads conjugated with IgG (#13773; Santa Cruz Biotechnology, Beijing, China) and green fluorescent protein (GFP; #48704; SAB, CA, USA) antibodies overnight at 4°C. The samples were isolated immunoprecipitated RNA and protein. Finally, the isolated protein was analyzed through protein mass spectrometry (Zhongke new life Biotechnology Co, Ltd., Zhejiang, China).

Quantitative Real-Time PCR

Total RNA was extracted from cells or samples using TRIzol reagent (Vazyme, Nanjing, China). Real-time PCR was performed using GoTaq®qPCR Master Mix (Promega), and specimens were detected using the StepOne Plus system (Applied Biosystems, Foster City, CA, USA). GAPDH was presented as an internal control. The primer sequences comprised MAGI2-AS3 forward: TGGTGATGACATGCCTACAGC; MAGI2-AS3 reverse: AGTGTGAAGGTAGGGAGTCTA; DNMT1 forward: CCTAGCCCCAGGATTACAAGG; DNMT1 reverse: ACTCATCCGATTTGGCTCTTTC; SPT6 forward: AGGGTGAAATCCGAGTGCG; SPT6 reverse: GGTGGCTGCTTTCTAGCTCA. The relative expression level was analyzed by the $2^{-\Delta\Delta C_t}$ method. The primers are listed in Supplemental Tables S1 and S2.

RNA Immunoprecipitation

RNA immunoprecipitation (RIP) for SPT6 protein was performed using a Magna RNA-binding protein immunoprecipitation kit (Genesee Biotech) in accordance with the manufacturer's instructions. TU177 and AMC-HN-8 cell lysates were prepared with RIP lysis buffer and then incubated with anti-SPT6 antibody (#15616S; Cell Signaling Technology, Danvers, MA, USA) or normal Rabbit IgG (#HA1002; HUABIO, Hangzhou, China) at 4°C for 6 h with rotation. RNA-protein complexes were retrieved using magnetic beads and then washed 6 times using the cold RIP wash buffer. Beads were separated using a magnetic separator from the sample. The supernatant underwent protein and RNA extraction. Next, Western blotting and qPCR analysis were performed.

DNA Extraction and Sodium Bisulfite Treatment

Genomic DNA was extracted from frozen LSCC tissues and matched non-tumor tissues, and TU177 and AMC-HN-8 cells. Genomic DNA sodium bisulfite was modified using

Epitect Fast Bisulfite Conversion Kits (Qiagen, Duesseldorf, Germany) in accordance with the manufacturer's protocol. Then the DNA methylation patterns were detected.

Bisulfite Genomic Sequencing Method

The distribution of methylated CpG sites of MAGI2-AS3 in TU177, AMC-HN-8 cell lines, two pairs of LSCC tissues, and matched non-tumor tissues was identified through the Bisulfite Genomic Sequencing (BGS) assay. The methylation condition of the CpG sites of three regions of MAGI2-AS3 was examined, respectively, and the result was from -886 to -530 bp, from -173 to 288 bp, and from 743 to 941 bp for the distal region, the first exon region, and the second exon region, respectively. Fifty nanograms of bisulfite-modified DNA was amplified using PCR, and the products were inserted into pGEM-T vectors (Promega, USA), and the above specimens were sequenced (Sangon Biotech). The primers are listed in Supplemental Table S3.

Methylation-Specific PCR Method

The methylation status of the distal CpG island region, the first exon region, and the second exon region of MAGI2-AS3 was analyzed, respectively, using the methylation-specific polymerase (MSP) method, and the results were from -592 to -461 bp, from -2 to 161 bp, and from 560 to 1,018 bp for the distal region, the first exon region, and the second exon region, respectively. MSP products would be further analyzed on 2% agarose gel using ethidium bromide staining and were considered for methylation if a visible band was examined. The reactions were performed in duplicate with the respective sample. The primers are listed in Supplemental Table S3.

Hematoxylin and Eosin and Immunohistochemical Staining

Paraffin-embedded LSCC tissues were cut into 4 μ m sections, deparaffinized, rehydrated, and then stained with hematoxylin and eosin (H&E). For antigen retrieval, the sections were heated at 95°C in ethylenediaminetetraacetic acid (EDTA) antigen retrieval solution (pH = 9.0), and the peroxidase activity was quenched for 10 min using 3% hydrogen peroxide. Next, the sections were incubated overnight using primary antibodies at 4°C. After being washed with phosphate-buffered saline (PBS), the sections were incubated with goat anti-rabbit IgG for 10 min and then stained with 3,3'-diaminobenzidine (DAB; Maixin, Biotech, Fuzhou, China). All sections were dehydrated and sealed after hematoxylin counterstaining. All images were captured under a light microscope.

Subcellular Fractionation

RNA from the nucleus or cytoplasm of cell lines was isolated by the PARIS™ Kit Protein and RNA Isolation System (Invitrogen). The qPCR method was used to detect the

expression level of MAGI2-AS3 in the cytoplasm and nucleus. Nuclear control and cytoplasmic control used were U6 and GAPDH, respectively.

Lentiviral Transduction and Tumor Xenograft Experiments

The human MAGI2-AS3 gene was cloned into the lentivirus vector CV146A. The lentiviral vector was transiently transfected into 293T cells. The viral supernatant fluid was acquired for subsequent experiments. Only TU177 cells were employed in animal experiments to avoid unnecessary animal killing. A total of 2×10^5 TU177 cells were infected with lenti-MAGI2-AS3 or lenti-Blast in the presence of 8 mg/ml polybrene (Solarbio). The stable cell lines were selected with blasticidin (Solarbio) for 10–14 days. All animal tests gained approval from the Committee on the Ethics of Animal Experiments of Hebei Medical University. Subsequently, 5- to 6-week-old BALB/c male nude mice were purchased from Charles River (Beijing, China). Mice in the experimental groups were randomly assigned to two groups, with 10 in the respective group. In the subcutaneous tumor xenograft experiment, a total of 5×10^6 cells were hanged in 200 μ l of serum-free 1640 and subcutaneously injected into the right flank of each mouse. The tumor growth was examined every 3–4 days after the initial 7 days. Tumor volume was obtained as follows: volume = (length \times width²)/2. Then, the animals were sacrificed, and the tumors were dissected and weighed after 4 weeks. Next, histological analysis was conducted.

Statistical Analysis

Statistical analysis was conducted using SPSS 17.0 software (SPSS, Chicago, IL, USA), and images were captured using GraphPad Prism 7 software (La Jolla, CA, USA). The significance of the differences between groups was assessed through a paired two-tailed Student's *t* test or chi-square test. The condition of gene methylation between different groups was studied through the chi-square test. Data are expressed as mean \pm standard deviation (SD). $P < 0.05$ indicated a difference that achieved statistical significance (* $P < 0.05$, ** $P < 0.01$).

Results

The Expression and Clinicopathological Relationship of MAGI2-AS3 in LSCC

To investigate the function of lncRNAs in the development of LSCC, the expression signatures in LSCC were probed using microarray analysis of four pairs of LSCC tissues and adjacent non-tumor tissues (Fig. 1A). P value < 0.05 and fold change < 0.5 were used as the cut-off criteria. MAGI2-AS3 was selected for further study. As indicated by

Gene Expression Profiling Interactive Analysis (GEPIA), MAGI2-AS3 was also expressed at a different level in different normal and tumor tissues (Fig. 1B). On that basis, MAGI2-AS3 expression was examined in 61 paired LSCC tissues and matched non-tumor tissues using qPCR to study the expression of MAGI2-AS3 and its clinical significance. The details of the clinicopathological characteristics are listed in Table 1. As indicated by the data, MAGI2-AS3 expression in LSCC tissues was significantly lower than the paired adjacent non-tumor tissues (Fig. 1C), consistent with our previous prediction. Moreover, MAGI2-AS3 expression was significantly lower in human LSCC cells (TU177 and AMC-HN-8) than normal epithelial cell 293T (Fig. 1D).

Next, the correlation of MAGI2-AS3 expression with clinicopathological features was examined. The expression of MAGI2-AS3 was positively correlated with cervical lymph node metastasis ($P = 0.047$) and TNM stages ($P = 0.022$), as indicated by the result of correlation analysis. However, no significant correlation was found between MAGI2-AS3 expression and other factors (eg, age [$P = 0.548$], smoking [$P = 0.625$], drinking [$P = 0.730$], and pathological differentiation [$P = 0.114$]) (Fig. 1E). The diagnostic efficacy of MAGI2-AS3 in LSCC screening was assessed using a receiver operating characteristic (ROC) curve. The area under the curve (AUC), diagnostic specificity and sensitivity of MAGI2-AS3, and T stage, N stage, pathological differentiation—TNM stages (0.675, 76.67%, 58.33%), (0.7373, 77.97%, 69.49%), (0.6293, 81.03%, 44.83%), and (0.55, 76.67%, 33.33%)—were used, respectively (Fig. 1F–J). As revealed by the above findings, MAGI2-AS3 may be critical to the progression of LSCC, and it is considered a new diagnostic biomarker.

MAGI2-AS3 Silencing Promoted Aggressive Cancer-Associated Phenotypes

In this context, to identify the biological function of MAGI2-AS3 in LSCC cells, TU177 (human LSCC cell line) and AMC-HN-8 (Asian Medical Center-Head and Neck cancer-8, human LSCC cell line, deriving from metastatic location: lymph node) were used. MAGI2-AS3 overexpression plasmid was transfected into TU177 and AMC-HN-8 cells. The overexpression efficiency was identified and detected (Supplemental Fig. S1A), and MAGI2-AS3 expression was markedly overexpressed in oe-MAGI2-AS3-transfected cells compared with pcDNA3.1-transfected cells (Fig. 2A). In this regard, to assess the effect of MAGI2-AS3 on cell proliferation, the MTS assay was used to detect the viability of TU177 and AMC-HN-8 cells at 0, 24, 48, 72, and 96 h, and the results showed that MAGI2-AS3 significantly inhibited the viability of TU177 and AMC-HN-8 cells (Fig. 2B and C). We further obtained the clonogenic ability of MAGI2-AS3 overexpression plasmid-transfected TU177 and AMC-HN-8 cells with MAGI2-AS3 overexpression plasmid followed by crystal violet staining and counting at 12 days after transfection.

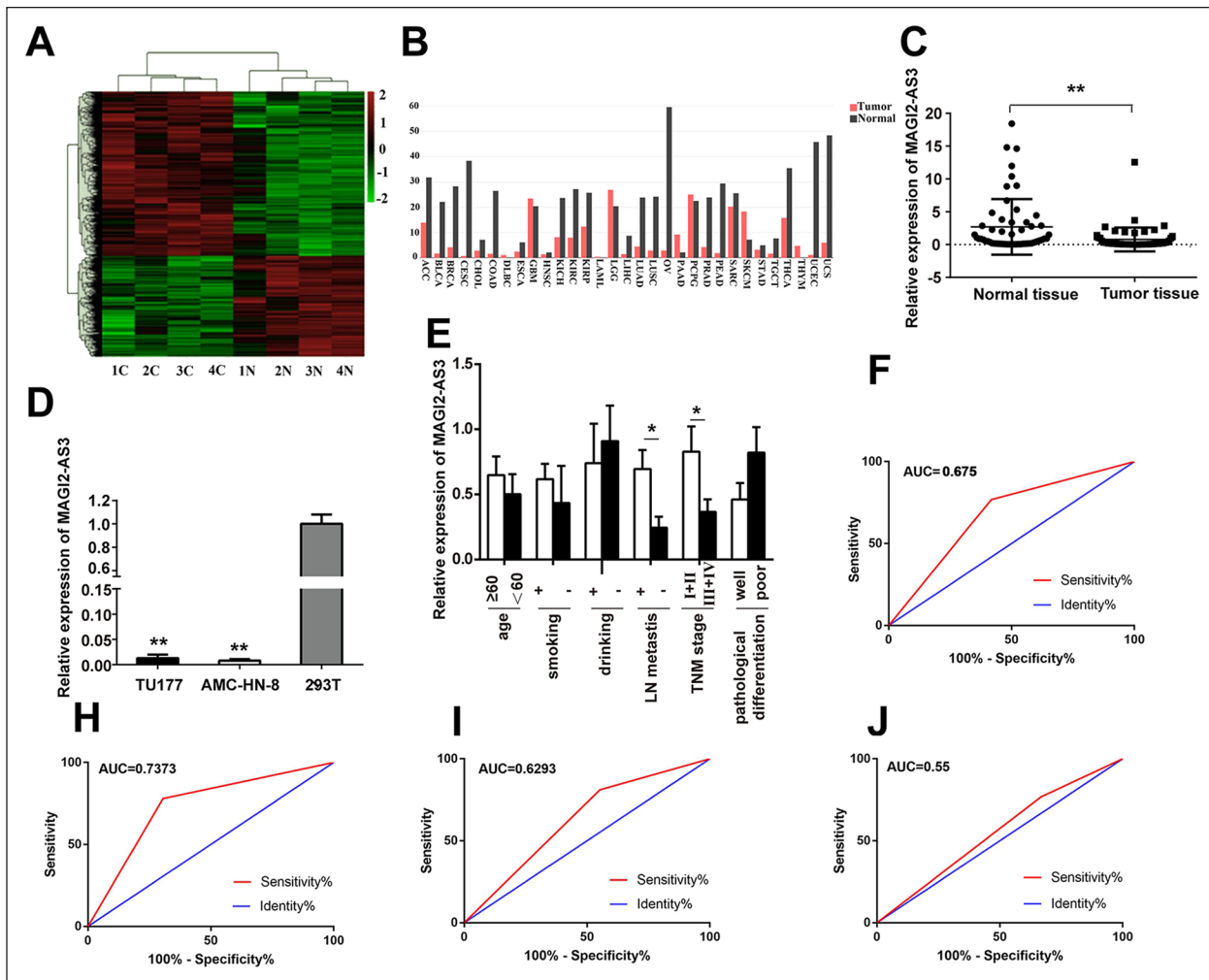


Figure 1. MAGI2-AS3 was downregulated in LSCC. (A) Heatmap diagram of lncRNA expression in four pairs of LSCC tissues and matched non-tumor tissues. (B) Relative expression of MAGI2-AS3 in various tumor types in the GEPIA data set. (C) Relative expression levels of MAGI2-AS3 in 61 pairs of LSCC tissues and matched non-tumor tissues. (D) Relative expression levels of MAGI2-AS3 in LSCC cells. (E) Relative expression of MAGI2-AS3 in different subgroups. (F, J) ROC analysis of the prognostic sensitivity and specificity for LSCC patients and general people. Data are presented as mean \pm SD from three independent experiments. * $P < 0.05$ and ** $P < 0.01$. MAGI2-AS3: MAGI2 antisense RNA 3; LSCC: laryngeal squamous cell carcinoma; lncRNAs: long noncoding RNAs; LN: lymph node; GEPIA: Gene Expression Profiling Interactive Analysis; ROC: receiver operating characteristic; ACC: adrenocortical carcinoma; BLCA: bladder urothelial carcinoma; BRCA: breast invasive carcinoma; CESC: cervical squamous cell carcinoma and endocervical adenocarcinoma; CHOL: cholangiocarcinoma; COAD: colon adenocarcinoma; DLBC: lymphoid neoplasm diffuse large B cell lymphoma; ESCA: esophageal carcinoma; GBM: glioblastoma multiforme; HNSCC: head and neck squamous cell carcinoma; KICH: kidney chromophobe; KIRC: kidney renal clear cell carcinoma; KIRP: kidney renal papillary cell carcinoma; LAML: acute myeloid leukemia; LGG: brain lower grade glioma; LIHC: liver hepatocellular carcinoma; LUAD: lung adenocarcinoma; LUSC: lung squamous cell carcinoma; MESO: mesothelioma; OV: ovarian serous cystadenocarcinoma; PAAD: pancreatic adenocarcinoma; PCPG: pheochromocytoma and paraganglioma; PRAD: prostate adenocarcinoma; READ: rectum adenocarcinoma; SARC: sarcoma; SKCM: skin cutaneous melanoma; STAD: stomach adenocarcinoma; TGCT: testicular germ cell tumors; THCA: thyroid carcinoma; THYM: thymoma; UCEC: uterine corpus endometrial carcinoma; UCS: uterine carcinosarcoma; UVM: uveal melanoma.

As indicated by the results, the colony-forming ability of TU177 and AMC-HN-8 cells was significantly reduced by MAGI2-AS3 overexpression (Fig. 2D). Furthermore, the effects of MAGI2-AS3 on the migration and invasion of LSCC cells were studied by wound-healing and transwell assays. Upregulated expression of MAGI2-AS3 following

transfection with TU177, AMC-HN-8/oe-MAGI2-AS3 significantly inhibited the migration and invasion of TU177 and AMC-HN-8 cells, as revealed by the results of the wound-healing (Fig. 2E and F) and transwell assays (Fig. 2G and H). In brief, overexpression of MAGI2-AS3 significantly inhibited cell proliferation, migration, and invasion of cells.

Table 1. Information and Clinicopathological Data of the 61 Pairs of Tumor and Adjacent Non-Tumor Tissues.

| Characteristics | n (%) |
|-------------------------------------|------------|
| Sex | |
| Male | 61 (100.0) |
| Female | 0 (0.0) |
| Age(years) | |
| <60 ^a | 18 (29.5) |
| ≥60 | 43 (71.5) |
| Smoking | |
| No | 6 (9.8) |
| Yes | 55 (90.2) |
| Alcohol consumption | |
| No | 19 (31.1) |
| Yes | 42 (68.9) |
| TNM stage | |
| I + II | 24 (39.3) |
| III + IV | 37 (60.7) |
| Cervical lymph node metastasis | |
| No | 41 (67.2) |
| Yes | 20 (32.8) |
| Pathological differentiation degree | |
| Well | 38 (62.3) |
| Moderate/poor | 23 (37.7) |

^aMedian age of the 61 patients. LSCC: laryngeal squamous cell carcinoma; TNM: tumor, node, metastasis.

MAGI2-AS3 Suppressed N-Cadherin and Vimentin in TUI177 and AMC-HN-8 Cells

The cellular localization of lncRNAs takes on a critical significance to functional investigations, such that the subcellular location of MAGI2-AS3 in cells was first scanned and examined. The result of lncAtlas (<http://lncatlas.crg.eu/>) indicated that MAGI2-AS3 was distributed primarily in the nucleus of HepG2 (human hepatocellular carcinoma cells) and human umbilical vein endothelial cells (HUVEC), whereas it was distributed in the cytoplasm of human endometrial stromal cells (hESC) (Supplemental Fig. S1B). In this study, results showed that MAGI2-AS3 was present in both the cytoplasm and nucleus but was more concentrated in the nucleus of TUI177 and AMC-HN-8 cells (Fig. 3A and B). EMT-associated markers (E-cadherin, N-cadherin, Vimentin, β -catenin, Zeb1, Snail, and Twist) were detected to study the molecular mechanism in depth. As depicted in Fig. 3C, TUI177 cells transfected with oe-MAGI2-AS3 indicated that the expression level of N-cadherin, Vimentin, Zeb1, and Snail was decreased by qPCR. As depicted in Fig. 3D, the expression of N-cadherin and Vimentin was lower in MAGI2-AS3-transfected AMC-HN-8 cells, and AMC-HN-8 also had the upregulated expression level of E-cadherin. At the same time, Western blotting revealed that overexpressing

MAGI2-AS3 was downregulated by Vimentin and N-cadherin expression levels, whereas E-cadherin expression level remained unchanged (Fig. 3E and F). In addition, after 5-Aza-dC treatment, Western blotting indicated that demethylation of the CpG island in the promoter of MAGI2-AS3 downregulated the expression of N-cadherin and Vimentin in TUI177 and AMC-HN-8 cells (Fig. 3G and H). As revealed by the above results, MAGI2-AS3 suppressed the mesenchymal phenotype by regulating N-cadherin and Vimentin.

Gene Promoter Hypermethylation Caused MAGI2-AS3 Downregulation in LSCC Tissues, TUI177, and AMC-HN-8 Cells

A schematic representation of the genomic organization of MAGI2-AS3 is presented in Fig. 4A to study the upstream mechanism of MAGI2-AS3. Furthermore, as depicted in Fig. 4B, MAGI2-AS3 had the three large CpG islands by MethPrimer (<http://www.urogene.org/>) analysis. After the cells were administrated with 5-Aza-dC, the expression levels of MAGI2-AS3 were significantly upregulated in TUI177 and AMC-HN-8 cell lines (Fig. 4D). Furthermore, the proliferation abilities of TUI177 and AMC-HN-8 cells were examined through a wound-healing assay, and the result indicated that the proliferation abilities were significantly reduced (Supplemental Fig. S1C). As indicated by the results, MAGI2-AS3 expression was likely to be regulated by DNA methylation. To further prove this result, frequent hypermethylation of the CpG islands of MAGI2-AS3 was examined by BGS in TUI177 and AMC-HN-8 cell lines and two pairs of LSCC tissues. After bisulfite DNA modification, methylated cytosine residues remained unchanged at CpG sites, whereas unmethylated cytosine residues were converted to thymine (Fig. 4C). As depicted in Fig. 3F, region 3 of the CpG island of MAGI2-AS3 exhibited a hypermethylation pattern in cancer cell lines. It is noteworthy that two pairs of LSCC tissues were selected in accordance with the expression level of MAGI2-AS3. In tumor tissues, the sites of region 3 of CpG island were hypermethylated, and in matched non-tumor tissues, region 3 of the CpG island was nearly unmethylated. As depicted in Fig. 4E, the TUI177 and AMC-HN-8 cell lines were all methylated in three regions of the CpG island, indicated by MSP. In LSCC cells before 5-Aza-dC treatment, three regions of MAGI2-AS3 showed significant methylation, and the methylation condition was reversed after 5-Aza-dC treatment. In 20 pairs of tumor tissues and matched non-tumor tissues, the rate of hypermethylation of region 3 of CpG island in tumor tissues was significantly higher than matched non-tumor tissues (Fig. 4G).

As depicted in Fig. 4H, in 20 tumor tissues, samples with methylation in region 3 displayed significantly lower

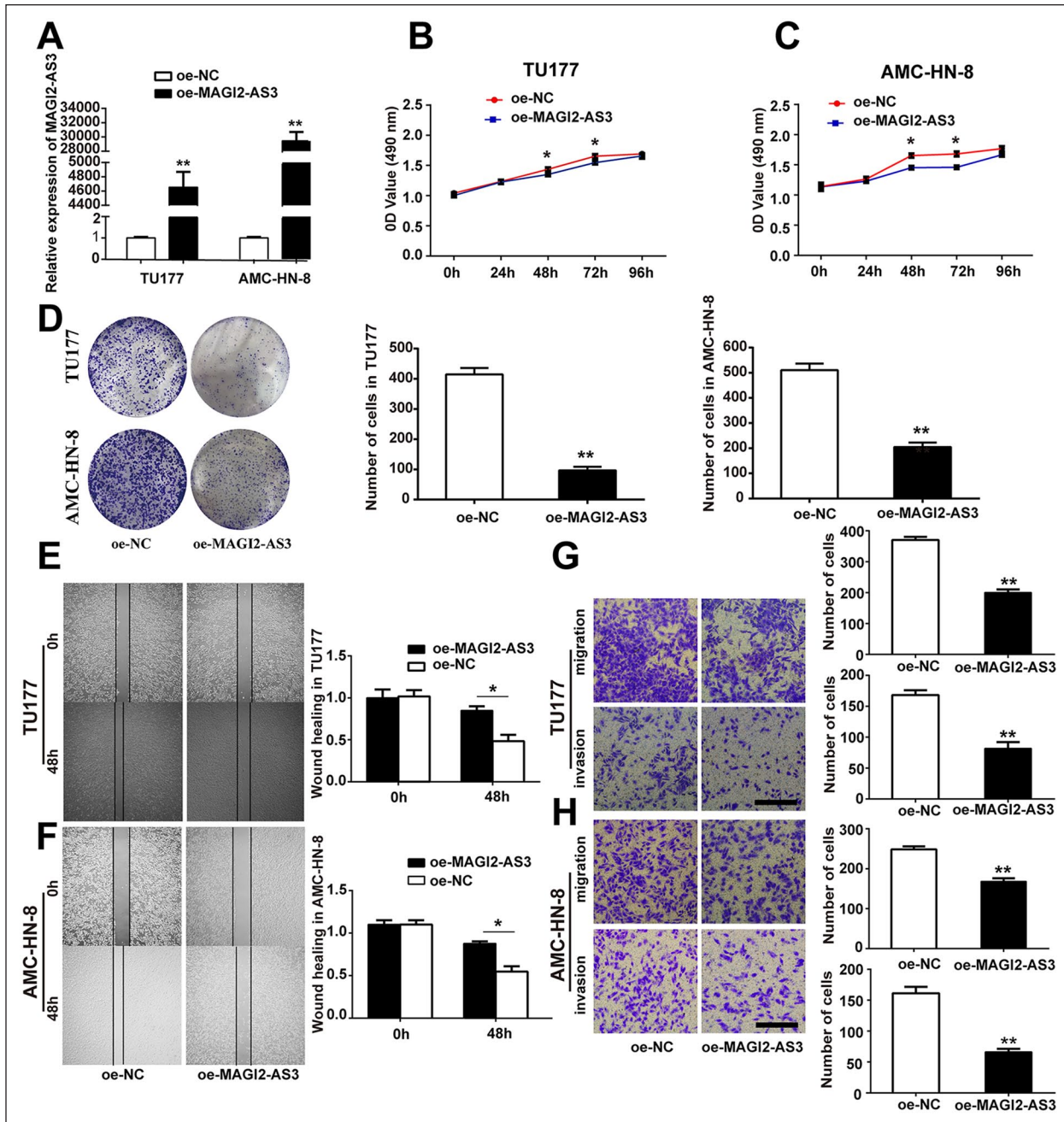


Figure 2. Functional analysis of MAGI2-AS3 in TUI77 and AMC-HN-8 cells. (A) The expression levels of MAGI2-AS3 in TUI77 and AMC-HN-8 transfected with pcDNA3.1-MAGI2-AS3 and pcDNA3.1. (B, C) Proliferation of TUI77 and AMC-HN-8 cells transfected with pcDNA3.1-MAGI2-AS3 was examined by the MTS assay. (D) Overexpression of MAGI2-AS3 significantly suppresses cell growth in a colony formation assay. (E, F) The effect of MAGI2-AS3 on migration was assessed using a scratch assay. (G, H) Migration and invasion abilities of the TUI77 and AMC-HN-8 cell lines, following overexpression of MAGI2-AS3 in the transwell assay. Scale bar, 100 μ m. Data are presented as mean \pm SD from three independent experiments. * $P < 0.05$, ** $P < 0.01$. MAGI2-AS3: MAGI2 antisense RNA 3; oe-MAGI2-AS3: pcDNA3.1-MAGI2-AS3; oe-NC: pcDNA3.1 vector. AMC-HN-8: Asian Medical Center-Head and Neck cancer-8.

expression levels of MAGI2-AS3 ($P < 0.05$). In both region 1 and region 2, the methylation showed no correlation with MAGI2-AS3 expression ($P > 0.05$). In further analysis, hypermethylation of region 3 was correlated with drinking,

pathological differentiation, and TNM stage (Table 2). The above findings revealed that hypermethylation in the CpG region close to the transcriptional start site of MAGI2-AS3 led to a significant reduction in MAGI2-AS3.

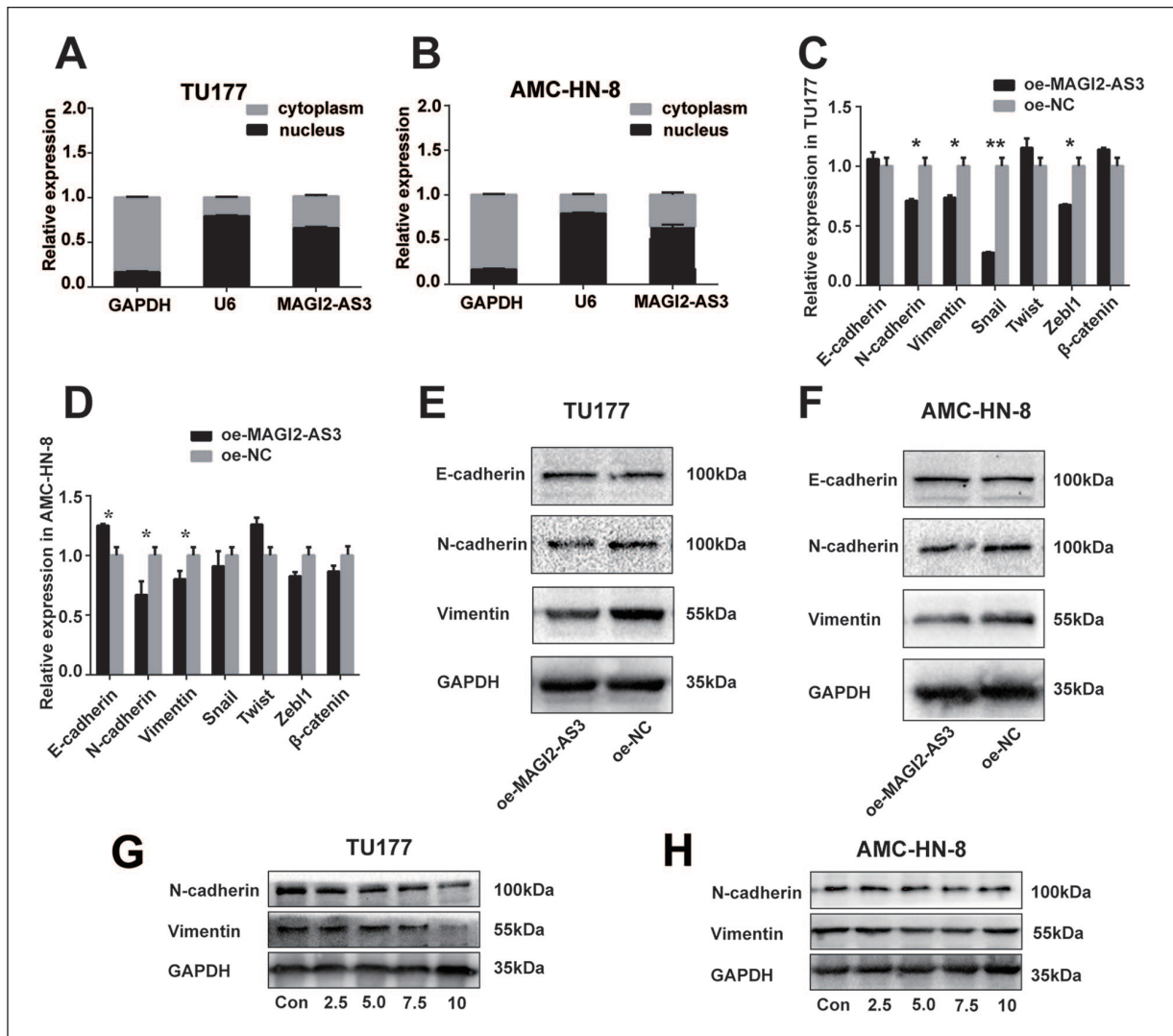


Figure 3. MAGI2-AS3 suppressed EMT *in vitro*. (A, B) Expression levels of MAGI2-AS3 in nuclear and cytoplasmic fractions of TUI77 and AMC-HN-8 cells were detected by qPCR. GAPDH: cytoplasmic control; U6: nuclear control. (C, D) Overexpression of MAGI2-AS3 increased the expression of EMT-associated markers detected by the qPCR method. (E, F) Relative protein expression levels of E-cadherin, N-cadherin, and Vimentin were assessed by Western blotting analysis in TUI77/overexpression-MAGI2-AS3, AMC-HN-8/overexpression-MAGI2-AS3, and control cells. (G, H) After TUI77 and AMC-HN-8 cells were administrated with different doses (2.5, 5, 7.5, 10 μ mol/L) of 5-Aza-dC, N-cadherin and Vimentin were detected by Western blotting. Data are presented as mean \pm SD from three independent experiments. * P < 0.05, ** P < 0.01. qPCR: quantitative polymerase chain reaction; EMT: epithelial-mesenchymal transition; AMC-HN-8: Asian Medical Center-Head and Neck cancer-8; MAGI2-AS3: MAGI2 antisense RNA 3.

DNMT1 Upregulation-Mediated MAGI2-AS3 Promoter Hypermethylation Inhibited Cell Proliferation, Migration, and Invasion In Vitro

DNMT1 knockdown efficiency was detected to study the mechanism of MAGI2-AS3 promoter hypermethylation in depth, and the expression was downregulated in sh-DNMT1 compared with pGeneSil-1 vector through qPCR (Supplemental Fig. S1D). Compared with that in the control group, MAGI2-AS3 expression of TUI77 and AMC-HN-8 cells was significantly upregulated in the sh-DNMT1 group (Fig. 5A). Meanwhile, the viability of TUI77 and

AMC-HN-8 cells was examined through the MTS assay; silencing DNMT1 significantly inhibited the viability of TUI77 and AMC-HN-8 cells, as indicated by the results (Fig. 5B and C). Furthermore, the effects of the promoter region of MAGI2-AS3 on the migration and invasion of LSCC cells were studied through wound-healing (Fig. 5D and E) and transwell assays (Fig. 5F and G). The depletion of DNMT1 significantly decreased cell migration and invasion ability. Data suggested low MAGI2-AS3 expression, such that the invasion and metastasis of LSCC cells were facilitated by affecting the EMT process, probably due to hypermethylation of MAGI2-AS3 in its promoter region.

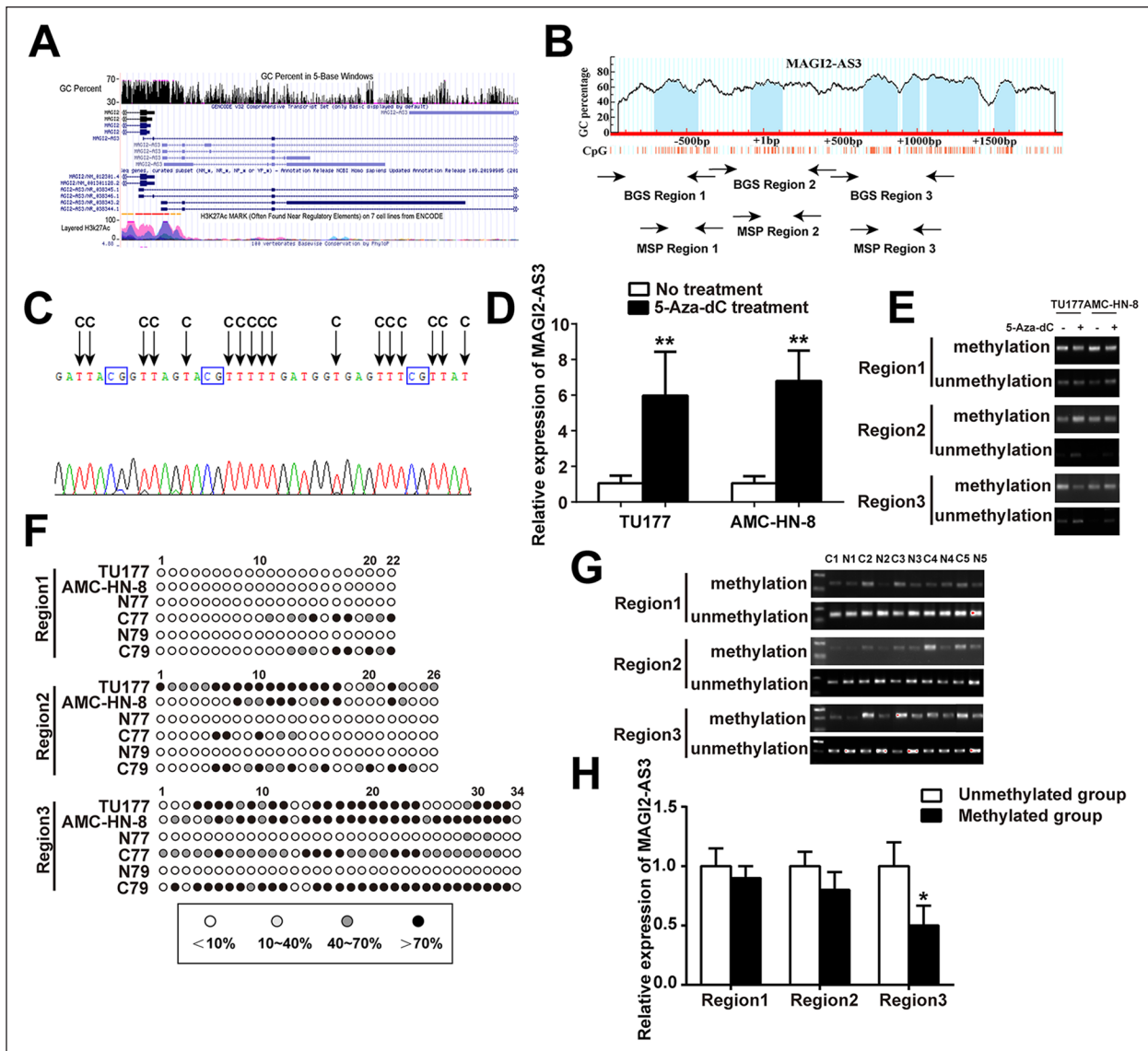


Figure 4. Methylation mechanisms of inactivation of MAGI2-AS3 in LSCC. (A) Location, MAGI2-AS3 cited from UCSC. (B) Schematic structure of MAGI2-AS3 CpG islands predicted by MethPrimer. (C) Schematic of cytosine changed after bisulfite DNA modification. (D) Relative expression levels of MAGI2-AS3 in 5-Aza-dC-treated two LSCC cell lines. (F) High-resolution mapping of the methylation status of every CpG site in MAGI2-AS3 CpG islands in two LSCC cell lines and two pairs of LSCC tissues obtained by BGS. Each CpG site is shown at the top row as an individual number. The color of circles for each CpG site represents the percentage of methylation. (E, G) The methylation status of three regions of MAGI2-AS3 detected by MSP analysis in two LSCC lines with or without 5-Aza-dC treatment and LSCC tissues versus matched non-tumor tissues. (H) Relative expression of MAGI2-AS3 in tumor tissues with and without methylation of the three regions. Data are presented as mean \pm SD from three independent experiments. * $P < 0.05$, ** $P < 0.01$. MAGI2-AS3: MAGI2 antisense RNA 3; oe-MAGI2-AS3: pcDNA3.1-MAGI2-AS3; oe-NC: pcDNA3.1 vector. LSCC: laryngeal squamous cell carcinoma; USSC: University of California Santa Cruz; BGS: bisulfite genomic sequencing; MSP: methylation-specific polymerase; AMC-HN-8: Asian Medical Center-Head and Neck cancer-8.

RNA-Binding Protein SPT6 Was Identified to Mediate the Inhibition of MAGI2-AS3 on Proliferation, Migration, and Invasion of Cells

To explore the downstream mechanism underlying MAGI2-AS3, the MS2-12X-dependent RNA pull-down assay was first performed (Fig. 6A), and then the MAGI2-AS3-binding proteins were detected through mass spectrometry analysis.

As indicated by the result, several proteins significantly enriched MAGI2-AS3, and fold change >10 and P value <0.05 served as the selection criteria. RNA-binding protein Knockdown reversed the oe-MAGI2-AS3 effect on TU177 and AMC-HN-8 cells, and the effect was examined. SPT6 was selected for further experiments (Fig. 6B), as indicated by the results of the rescue experiment and pieces of literature. The selective binding of SPT6 with MAGI2-AS3 was

Table 2. Methylation Status of MAGI2-AS3 in LSCC Tissues.

| Group | N | Methylation frequency | | | | | |
|------------------------------|----|-----------------------|-------|-----------|-------|-----------|-------|
| | | Region 1 | | Region 2 | | Region 3 | |
| | | n (%) | P | n (%) | P | n (%) | P |
| Age | | | | | | | |
| <60 | 4 | 3 | 0.494 | 2 | 0.822 | 2 | 0.431 |
| ≥60 | 16 | 9 | | 9 | | 11 | |
| Smoking | | | | | | | |
| Positive | 15 | 10 | 0.689 | 8 | 0.795 | 11 | 0.840 |
| Negative | 5 | 2 | | 3 | | 2 | |
| Drinking | | | | | | | |
| Positive | 12 | 8 | 0.456 | 7 | 0.714 | 10 | 0.003 |
| Negative | 8 | 4 | | 4 | | 3 | |
| Pathological differentiation | | | | | | | |
| Well | 8 | 4 | 0.456 | 3 | 0.199 | 3 | 0.035 |
| Moderate/poor | 12 | 8 | | 8 | | 10 | |
| TNM stage | | | | | | | |
| I + II | 11 | 6 | 0.582 | 4 | 0.064 | 5 | 0.042 |
| III + IV | 9 | 6 | | 7 | | 8 | |
| LN metastasis | | | | | | | |
| Positive | 7 | 6 | 0.085 | 5 | 0.279 | 3 | 0.128 |
| Negative | 13 | 6 | | 6 | | 10 | |
| Tissues | | | | | | | |
| Tumor | 20 | 12 (60.0) | 0.749 | 11 (55.0) | 1.0 | 13 (70.0) | 0.027 |
| Normal | 20 | 11 (55.0) | | 11 (55.0) | | 6 (30.0) | |

In 20 pairs of tumor tissues and matched non-tumor tissues, the rate of hypermethylation of region 3 of CpG island in tumor tissues was significantly higher than in normal tissues. In 20 tumor tissues, hypermethylation of MAGI2-AS3 was associated with drinking, moderate/poor pathological differentiation, and TNM stage. MAGI2-AS3: MAGI2 antisense RNA 3; LSCC: laryngeal squamous cell carcinoma; LN: lymph node; TNM: tumor, node, metastasis.

further supported by RIP results (Fig. 6C and D). The knock-down efficiency was examined, and SPT6 expression was downregulated in sh-SPT6 compared with pGeneSil-1 vector through qPCR (Fig. 6E). Plate colony formation and MTS assays indicated that the inhibition of the proliferation ability of MAGI2-AS3 overexpression was reversed by the exogenous downregulation of SPT6 expression (Fig. 6F–H). The same result was achieved through the wound-healing assay (Fig. 6I and J). In addition, the results of transwell migration and Matrigel invasion assays suggested that SPT6 knockdown partly rescued the loss of motility abilities of overexpressed-MAGI2-AS3 cell lines compared with the control group (Fig. 6K and L). The above results revealed a mechanism that MAGI2-AS3 inhibits cell proliferation, migration, and invasion through SPT6 promotion by binding to LSCC cells.

SPT6 Inhibited the Proliferation, Migration, and Invasion of TU177 and AMC-HN-8 Cells

SPT6 expression was knocked down and overexpressed using its shRNA and one overexpression plasmid in TU177 and AMC-HN-8 cells to examine the functional effect of SPT6 in LSCC cell lines. The overexpression efficiency of SPT6 was

examined through qPCR (Fig. 7A). The depletion of SPT6 resulted in a marked increase in the colony-forming ability of TU177 and AMC-HN-8 cells (Fig. 7B). Moreover, after wound-healing (Fig. 7C and D) and transwell assays (Fig. 7E and F) were performed, the result indicated that the interference with SPT6 significantly enhanced the migration and invasion abilities of LSCC cells. In contrast, the effect of ectopic SPT6 expression on the oncogenic phenotypes of TU177 and AMC-HN-8 cells was examined. On that basis, a clonogenic assay was performed, in which the colony formation ability was moderately reduced upon SPT6 overexpression to assess the effect of SPT6 on cell proliferation (Fig. 7B). Next, the effect of ectopic SPT6 expression on the ability to invade the Matrigel-coated membrane was examined, and the cell invasion ability was reduced (Fig. 7F). Moreover, SPT6 overexpression led to reduced cell migration ability (Fig. 7C–E). Accordingly, MAGI2-AS3 recruited and interacted with SPT6 to inhibit the proliferation, migration, and invasion of LSCC cells *in vitro*.

Overexpressed-MAGI2-AS3 Inhibited the Growth of Xenograft Tumors of LSCC Cells In Vivo

To verify the regulatory effect of MAGI2-AS3 on LSCC under *in vivo* conditions, an oeRNA lentiviral plasmid was

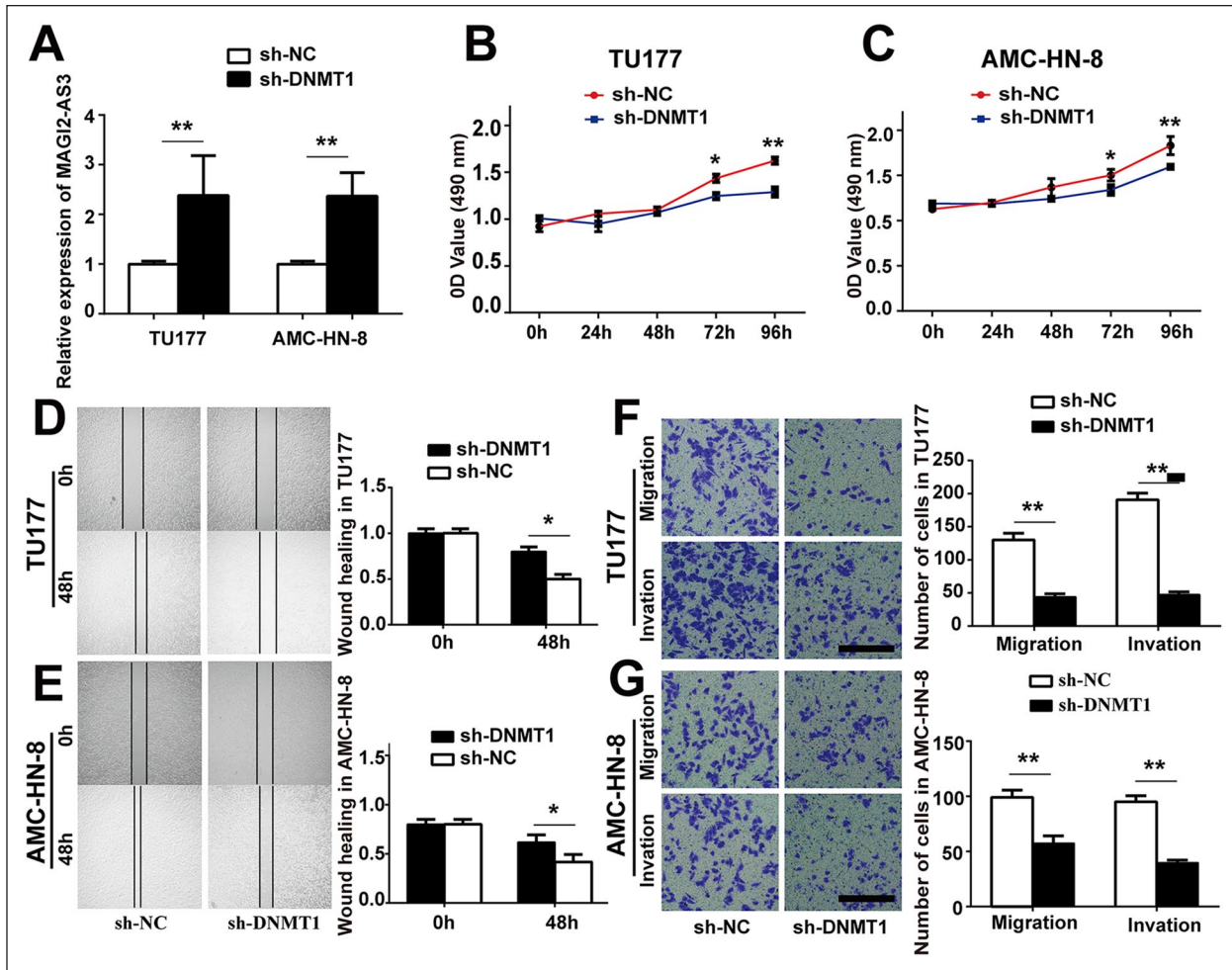


Figure 5. Functional analysis of DNMT1 in TUI77 and AMC-HN-8 cells. (A) TUI77 and AMC-HN-8 cells were transfected with sh-DNMT1 or pGeneSil-1 vector, and then MAGI2-AS3 expression was obtained by qPCR. (B, C) TUI77 and AMC-HN-8 cells were transfected with sh-DNMT1 or pGeneSil-1 vector; cell proliferation was detected by the MTS assay. (D, E) Proliferative capacity of TUI77 and AMC-HN-8 cells transfected with sh-DNMT1 or pGeneSil-1 vector was assessed by the wound-healing assay. (F, G) Effect of DNMT1 on the migration and invasion of TUI77 and AMC-HN-8 cells was assessed by transwell migration and invasion assays. Scale bar, 100 μ m. Data are presented as mean \pm SD of three independent experiments. *sh-NC versus sh-DNMT1. * $P < 0.05$, ** $P < 0.01$. MAGI2-AS3: MAGI2 antisense RNA 3; DNMT1: DNA methyltransferase 1; AMC-HN-8: Asian Medical Center-Head and Neck cancer-8; qPCR: quantitative polymerase chain reaction.

constructed that targeted MAGI2-AS3 and screened TUI77 cells following stable overexpression of MAGI2-AS3 (lenti-MAGI2-AS3). By qPCR, the overexpression efficiency of MAGI2-AS3 was confirmed (Fig. 8A). Next, xenograft tumor models of nude mice were built by subcutaneously injecting stably transfected TUI77 cells. The xenograft tumors formed by overexpressed-MAGI2-AS3 LSCC cells had a significantly smaller volume than those of the control group (lenti-Blast) (Fig. 8B–D), and the tumor weight was also significantly lower than the lenti-Blast group (Fig. 8E). The total RNA of xenograft tumors was extracted, and MAGI2-AS3, SPT6, and Ki67 expression was examined through qPCR.

The results verified that MAGI2-AS3 and SPT6 expressions were increased in the lenti-MAGI2-AS3 group compared with the control group (Fig. 8F and G). In contrast, the expression level of Ki67 was distinctly downregulated (Fig. 8H). Furthermore, H&E staining showed that overexpression of MAGI2-AS3 (lenti-MAGI2-AS3) significantly reduced the number of lesions (Fig. 8I). Immunohistochemical (IHC) staining indicated that the expression of proliferation marker Ki67, EMT marker N-cadherin, and Vimentin was downregulated in lenti-MAGI2-AS3 xenograft tumors (Fig. 8J). As revealed by the above results, MAGI2-AS3 can inhibit the malignant progression of LSCC *in vivo*.

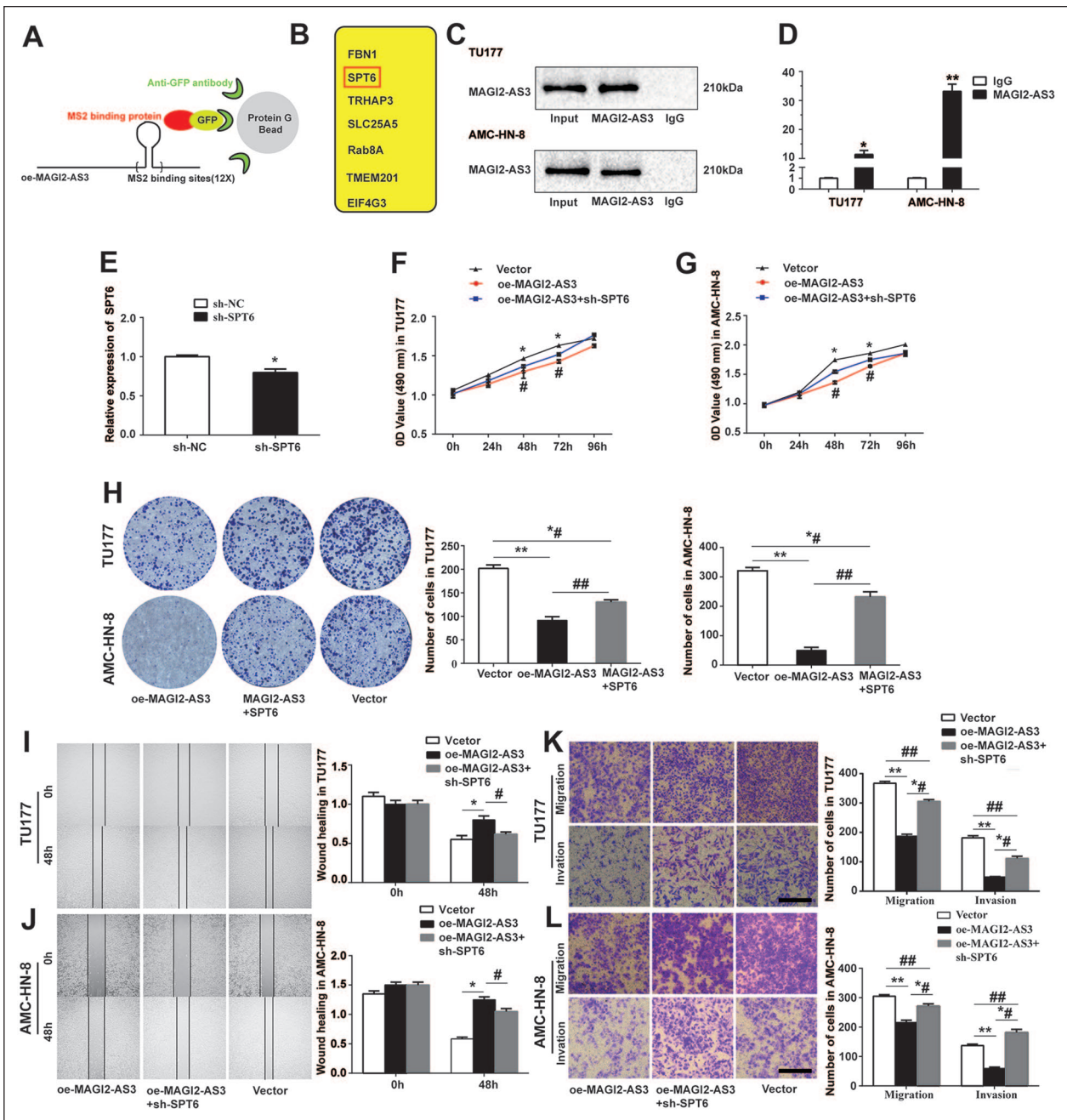


Figure 6. MAGI2-AS3 induced antitumor effects in LSCC cells by interacting with SPT6. (A) Schematic of the MS2-12X-dependent RNA pull-down experiments. (B) MAGI2-AS3-binding proteins by mass spectrometry analysis. (C) SPT6 identified specifically bind to MAGI2-AS3 by Western blotting. (D) RIP was performed to confirm the interaction of SPT6 and MAGI2-AS3. (E) The expression levels of SPT6 in the TU177 knockdown of SPT6. (F, G) TU177 and AMC-HN-8 cells were transfected with oe-MAGI2-AS3 or cotransfected with oe-MAGI2-AS3 and sh-SPT6. Cell proliferation was obtained by the MTS assay. (H) Colony formation assays were performed to assess the proliferative ability of TU177 and AMC-HN-8 cells transfected with oe-MAGI2-AS3 or cotransfected with oe-MAGI2-AS3 and sh-SPT6. Effects of oe-MAGI2-AS3 and sh-SPT6 on the migration and invasion of TU177 and AMC-HN-8 cells were assessed by the (I, J) wound-healing assay and (K, L) transwell migration and invasion assays. Scale bar, 100 μ m. Data are presented as mean \pm SD of three independent experiments. *Vector versus oe-MAGI2-AS3; #oe-MAGI2-AS3 versus oe-MAGI2-AS3+sh-SPT6; ## Vector versus oe-MAGI2-AS3+sh-SPT6. * $P < 0.05$, ** $P < 0.01$; # $P < 0.05$, ### $P < 0.01$; *# $P < 0.01$. MAGI2-AS3: MAGI2 antisense RNA 3; LSCC: laryngeal squamous cell carcinoma; SPT6: Suppressor Of Ty 6 Homolog; RIP: RNA Immunoprecipitation; AMC-HN-8: Asian Medical Center-Head and Neck cancer-8; GFP: green fluorescent protein.

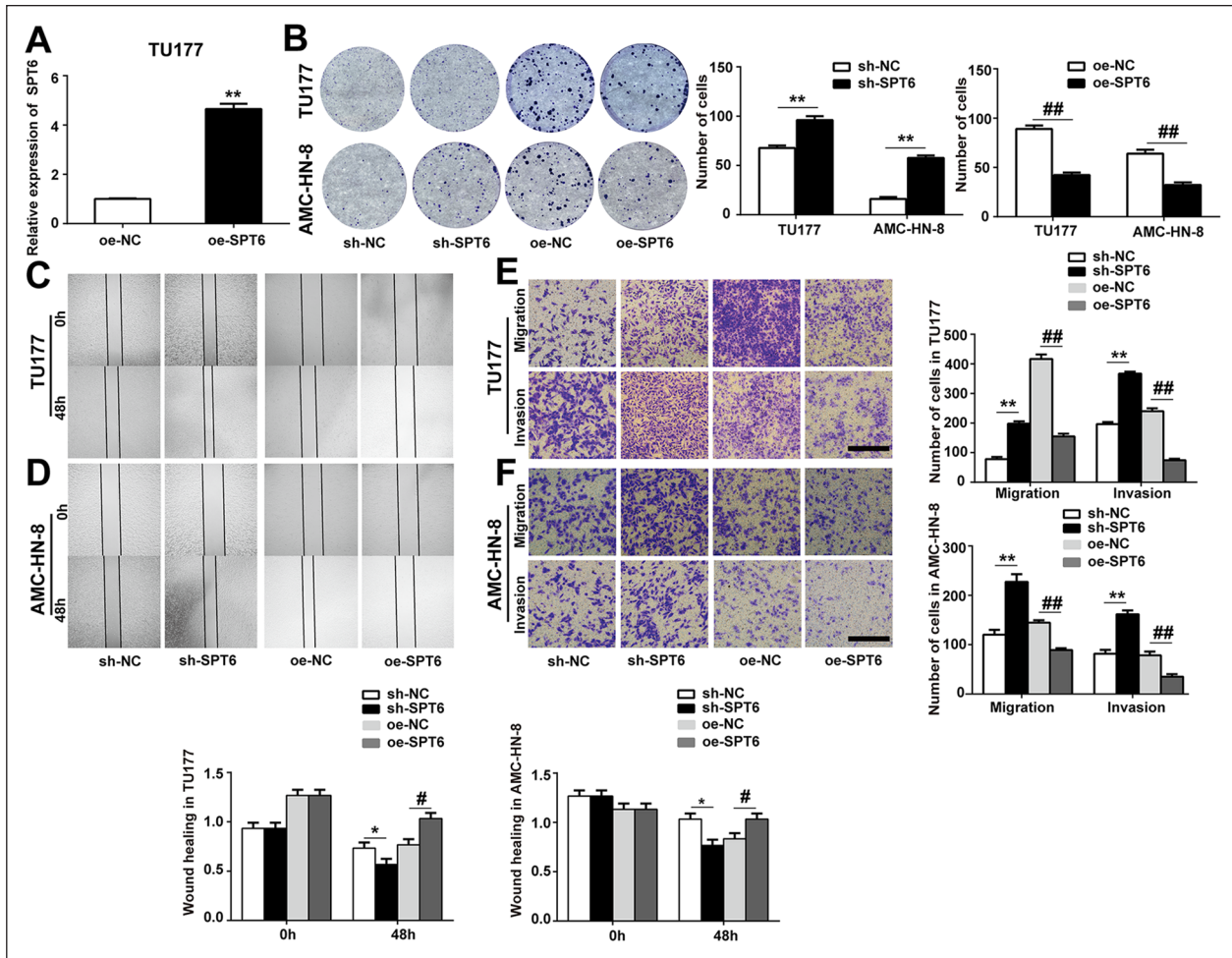


Figure 7. SPT6 regulated the proliferation, migration, and invasion of LSCC cells. (A) The expression levels of SPT6 in TU177 overexpressed SPT6. (B) The colony formation assay was performed for the proliferation of SPT6 regulating TU177 and AMC-HN-8 cells. (C, D) The wound-healing assay was performed for the migration of SPT6 regulating TU177 and AMC-HN-8 cells. (E, F) The transwell assay was performed for invasion and migration of SPT6 regulating TU177 and AMC-HN-8 cells. Scale bar, 100 μ m. Data are presented as mean \pm SD of three independent experiments. *sh-NC versus sh-SPT6; #oe-NC versus oe-SPT6. * $P < 0.05$, ** $P < 0.01$; # $P < 0.05$, ### $P < 0.01$; *## $P < 0.01$. SPT6: Suppressor Of Ty 6 Homolog; LSCC: laryngeal squamous cell carcinoma; AMC-HN-8: Asian Medical Center-Head and Neck cancer-8.

Discussion

In our study, we performed a microarray analysis of LSCC, matched non-tumor tissues, and established the lncRNA expression profiles of LSCC tissues. MAGI2-AS3, a 901-bp polyadenylated lncRNA, is located at 5q15 (GRCh 38/hg38 database, chr7:79452957-79471208, NCBI: 038346.1). Clinical specimen analysis indicated that MAGI2-AS3 was downregulated in LSCC tissues compared with matched non-tumor tissues. This change in MAGI2-AS3 levels showed a correlation with advanced TNM stage and lymph node metastasis. ROC curve confirmed the diagnostic specificity and sensitivity of MAGI2-AS3 in LSCC screening. Moreover, MAGI2-AS3 expression was significantly lower in human LSCC cells (TU177 and AMC-HN-8). The initial exploration also showed that MAGI2-AS3 declined in hepatocellular carcinoma and lung cancer and regulated the

malignant progression of tumor^{20,21}. All the above findings indicated that MAGI2-AS3 may be critical to LSCC progression, and it is expected to serve as a new biomarker for the early diagnosis of LSCC.

The present data indicated that overexpression of MAGI2-AS3 significantly decreased cell proliferation, migration, and invasion capacities in TU177 and AMC-HN-8 cells through MTS, colony formation, transwell, and wound-healing assays. *In vivo*, xenograft tumor models of nude mice were built by subcutaneously injecting stably transfected TU177 cells. The xenograft tumor volume and weight formed by overexpressed-MAGI2-AS3 LSCC cells were significantly smaller and lower than those of the control group. The important feature is proliferation marker Ki67 expression was downregulated in lenti-MAGI2-AS3 xenograft tumors. In general, EMT has been considered a major event in metastasis, drug

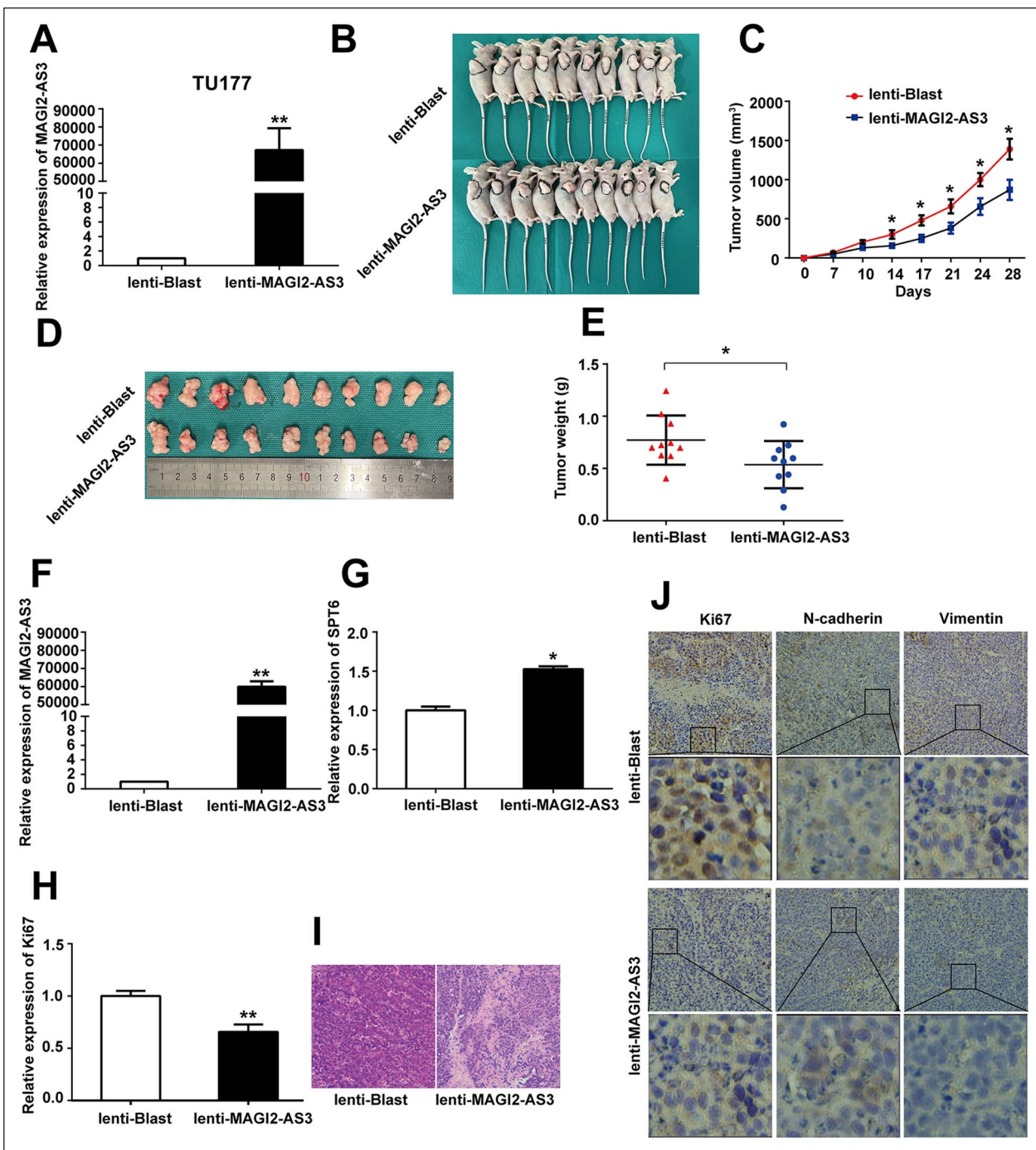


Figure 8. MAGI2-AS3 inhibited the tumor growth of LSCC cells *in vivo*. (A) The expression levels of MAGI2-AS3 in TUI77 stably overexpressed MAGI2-AS3 (lenti-MAGI2-AS3). (B, D) Nude mice were subcutaneously injected with negative control (lenti-Blast), and lenti-MAGI2-AS3 stably transfected TUI77 cells. After 28 days, tumors were dissected and imaged. (C) Starting from day 7 after injection, the tumor volume was examined every 3–4 days, and the tumor growth curve was plotted. (E) The tumor weight was obtained on the day the mice were killed. Data represent mean \pm SD ($n = 10$ each group). (F, H) The expression levels of MAGI2-AS3, SPT6, and Ki67 in xenograft tumors were obtained by qPCR. (I) H&E staining revealed the structure of xenograft tumors derived from oe-NC and oe-MAGI2-AS3 LSCC cells. Scale bar, 50 μ m. (J) Changes in Ki67, N-cadherin, and Vimentin expression in xenograft tumors were detected by IHC staining. Scale bar, 50 μ m. Data are presented as mean \pm SD from three independent experiments. * $P < 0.05$ and ** $P < 0.01$. LSCC: laryngeal squamous cell carcinoma; SPT6: Suppressor Of Ty 6 Homolog; AMC-HN-8: Asian Medical Center-Head and Neck cancer-8; IHC: immunohistochemistry; qPCR: quantitative polymerase chain reaction; MAGI2-AS3: MAGI2 antisense RNA 3.

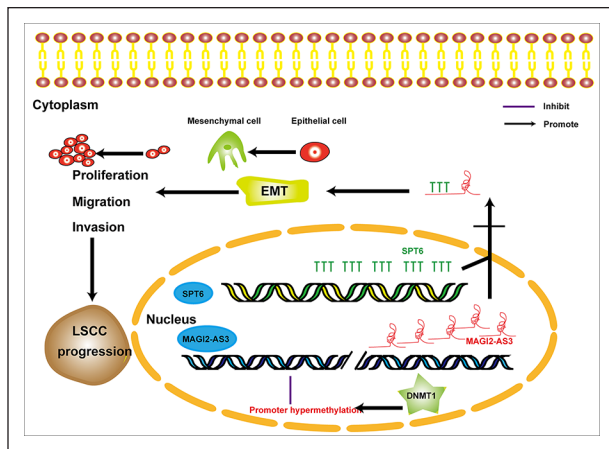


Figure 9. A proposed scheme of the roles and molecular mechanisms of MAGI2-AS3 in LSCC progression is presented. LSCC: laryngeal squamous cell carcinoma; EMT: epithelial-mesenchymal transition; SPT6: Suppressor Of Ty 6 Homolog; DNMT1: DNA methyltransferase I; MAGI2-AS3: MAGI2 antisense RNA 3.

resistance and disease recurrence although the concrete process of tumor metastasis and reappearance remains elusive^{22,23}. As revealed by the transformation of epithelial surface markers, especially E-cadherin, and the development of mesenchymal markers (eg, Vimentin and N-cadherin), cells have undergone the EMT process²⁴. The results of this study verified that over-expressing MAGI2-AS3 in TU177 and AMC-HN-8 cells significantly downregulated Vimentin and N-cadherin expression levels by qPCR and Western blotting. *In vivo*, N-cadherin and Vimentin expression detected by IHC staining was also downregulated in lenti-MAGI2-AS3 xenograft tumors. Huang et al.²⁵ have also suggested that lncRNA SGO1-AS1 inhibited transforming growth factor beta (TGF- β) production and prevented the EMT of gastric carcinoma (eg, the elevated levels of E-cadherin), whereas it downregulated Vimentin and N-cadherin expression and reduced the elongation of cell bodies. Moreover, the expression levels of EMT-induced transcription factors (eg, ZEB1, SNAI, and SLUG) were downregulated. In addition, after the cells were administrated with different doses of 5-Aza-dC, the result of Western blotting indicated that demethylation of the CpG island in the promoter of MAGI2-AS3 downregulated Vimentin and N-cadherin expression in TU177 and AMC-HN-8 cells. As mentioned above, the results confirmed that MAGI2-AS3 can serve as a tumor suppressor lncRNA by adjusting the EMT process through hypermethylation in LSCC.

Low expression of lncRNAs in LSCC has been extensively reported, whereas the reasons for the low expression have been rarely studied. Nuclear lncRNAs are beneficial to regulate numerous genes by changing the condition of DNA through histone modifications and DNA modifications or recruiting specific factors to the DNA at the transcriptional level. In humans, DNMT1 is responsible for maintaining the

existing methylation. Abnormal regulation of the enzyme expression leads to abnormal methylation²⁶. In the findings of this study, MAGI2-AS3 was mostly located in the nucleus of TU177 and AMC-HN-8 cells. After treatment with 5-Aza-dC, the expression levels of MAGI2-AS3 were significantly increased in TU177 and AMC-HN-8 cell lines. By BGS assays, region 3 of CpG island of TU177 and AMC-HN-8 indicated hypermethylation patterns in the promoters of MAGI2-AS3. In LSCC tissues, the sites of region 3 of CpG island were hypermethylated, and in matched non-tumor tissues, region 3 of CpG island was almost unmethylated. By MSP assays, in 20 pairs of tumor tissues and matched non-tumor tissues, the rate of hypermethylation of region 3 of CpG island in tumor tissues was significantly higher than that in matched non-tumor tissues. In 20 tumor tissues, the methylation in region 3 showed a lower expression level of MAGI2-AS3. However, there was no correlation between methylation and MAGI2-AS3 expression in region 1 and region 2. Hypermethylation of region 3 showed a correlation with drinking, moderate/poor pathological differentiation, and TNM stage.

The effects of the promoter region of MAGI2-AS3 on the proliferation, migration, and invasion of LSCC cells were studied through wound-healing, colony formation, and transwell assays. Knockdown of DNMT1 significantly inhibited cell proliferation, migration, and invasion. Wang et al.²⁷ determined DNA hypermethylation levels of DICER1-AS1 in the osteosarcoma according to The Cancer Genome Atlas (TCGA) data sets. Moreover, Pan et al.²⁸ confirmed that lncRNA UCA1 upregulation via DNA hypomethylation in the UCA1 promoter, which is mediated by DNMT1. As revealed by the above findings, the DNMT1 upregulation mediates MAGI2-AS3 downregulation caused by MAGI2-AS3 promoter hypermethylation in LSCC while enhancing the proliferation, migration, and invasion of LSCC cells.

The biological functions of the majority of lncRNAs remain unclear although several lncRNAs have been studied in depth. Recent studies demonstrated that most of the lncRNAs regulated a wide variety of biological activities through specific correlations with chromatin, such as interacting with corresponding RBPs^{29,30}. Accordingly, the identification of the potential lncRNA protein interaction (LPI) is vital in understanding lncRNAs' biological functions and mechanisms. lncRNAs fulfill their biological functions at least in part by interacting with distinctive proteins.

Moreover, we achieved a preliminary exploration of the regulatory mechanism of MAGI2-AS3 and SPT6 in LSCC. In this study, MAGI2-AS3 and SPT6 could interact directly, as indicated by the results of MS2-12X-dependent RNA pull-down and RNA immunoprecipitation assays. Several rescue experiments, including the MTS, plate colony formation, wound-healing, and transwell assays, were performed by cotransfecting oe-MAGI2-AS3 and sh-SPT6 in TU177 and AMC-HN-8 cells. SPT6 knockdown partly mediated the proliferation, migration, and invasion abilities

of overexpressed-MAGI2-AS3 cell lines compared with the control group. Furthermore, overexpressed-SPT6 inhibited the proliferation and metastasis of LSCC cells. Besides, MAGI2-AS3 suppressed the proliferation, migration, and invasion abilities of LSCC cells through interaction with SPT6.

MAGI2-AS3 genes known to bind RBPs have been reported. Jiang et al.³¹ have suggested that MAGI2-AS3 had high connections with RBPs and miRNAs in the pan-cancer network and the new role of a member of the pan-cancer RBP-ncRNA circuits hsa-miR-224-5p-MAGI2-AS3-MBNL2 in the EMT program. Subsequently, the abnormal expression of RBPs was closely correlated with the occurrence and development of malignant tumors; the RBP EIF4A3 was overexpressed in a considerable number of cancers and coordinated cell cycle and cell apoptosis^{32,33}. However, the RNA network exhibited a multilayered, multidirectional, multi-interactive, and multidimensional network architecture that is capable of coordinating cellular responses. Whether MAGI2-AS3 communicated with other miRNAs/mRNAs to form RNA regulatory networks should be verified in depth.

Conclusion

In brief, the more comprehensive molecular mechanism of MAGI2-AS3 was illustrated in this study. The data revealed that DNMT1 upregulation-mediated MAGI2-AS3 promoter hypermethylation led to downregulated MAGI2-AS3 expression in LSCC, thereby promoting the proliferation, migration, and invasion of LSCC cells by EMT. MAGI2-AS3 could play a part in antitumor effects via interacting with SPT6 (Fig. 9). The above findings offered fresh insights into the occurrence and progression of LSCC and indicated the potential of MAGI2-AS3 as a biomarker and therapeutic target for LSCC.

Author Contributions

Jiantao Wang and Baoshan Wang conceived and designed the analysis. Huan Cao and Jianwang Yang collected the data. Chuan Yang contributed data or analysis tools. Jiantao Wang, Miaomiao Yu, and Lei Yu performed the analysis. Jiantao Wang wrote the paper. Baoshan Wang and Wenxia Meng performed the validation.

Ethical Approval

This study was approved by the Ethics Committee of Hebei Medical University and the Second Hospital of Hebei Medical University.

Statement of Human and Animal Rights

All the experimental procedures involving patients were conducted in accordance with the Helsinki Declaration for human studies and approved by the ethics committee at Hebei Medical University (Hebei, China).

Statement of Informed Consent

Written informed consents were obtained from the patients for the collection and publication of clinical data.

Declaration of Conflicting Interests

The author(s) declared no potential conflicts of interest with respect to the research, authorship, and/or publication of this article.

Funding

The author(s) disclosed receipt of the following financial support for the research, authorship, and/or publication of this article: This study was supported by the National Natural Science Foundation of China (No: 81972553).

ORCID iD

Baoshan Wang  <https://orcid.org/0000-0002-2455-8338>

Supplemental Material

Supplemental material for this article is available online.

References

- Steuer CE, El-Deiry M, Parks JR, Higgins KA, Saba NF. An update on larynx cancer. *CA Cancer J Clin.* 2017;67(1):31–50.
- Siegel RL, Miller KD, Jemal A. Cancer statistics, 2019. *CA Cancer J Clin.* 2019;69(1):7–34.
- Zhao S, Zhang X, Chen S, Zhang S. Natural antisense transcripts in the biological hallmarks of cancer: powerful regulators hidden in the dark. *J Exp Clin Cancer Res.* 2020;39(1):187.
- Peng WX, Koirala P, Mo YY. LncRNA-mediated regulation of cell signaling in cancer. *Oncogene.* 2017;36(41):5661–67.
- Magistri M, Faghihi MA, St Laurent G 3rd, Wahlestedt C. Regulation of chromatin structure by long noncoding RNAs: focus on natural antisense transcripts. *Trends Genet.* 2012;28(8):389–96.
- Song K, Yu P, Zhang C, Yuan Z, Zhang H. The LncRNA FGD5-AS1/miR-497-5p axis regulates septin 2 (SEPT2) to accelerate cancer progression and increase cisplatin-resistance in laryngeal squamous cell carcinoma. *Mol Carcinog.* 2021;60(7):469–80.
- Meng W, Cui W, Zhao L, Chi W, Cao H, Wang B. Aberrant methylation and downregulation of ZNF667-AS1 and ZNF667 promote the malignant progression of laryngeal squamous cell carcinoma. *J Biomed Sci.* 2019;26(1):13.
- Yuan L, Tian X, Zhang Y, Huang X, Li Q, Li W, Li S. LINC00319 promotes cancer stem cell-like properties in laryngeal squamous cell carcinoma via E2F1-mediated upregulation of HMGB3. *Exp Mol Med.* 2021;53(8):1218–28.
- Li X, Xu F, Meng Q, Gong N, Teng Z, Xu R, Zhao M, Xia M. Long noncoding RNA DLEU2 predicts a poor prognosis and enhances malignant properties in laryngeal squamous cell carcinoma through the miR-30c-5p/PIK3CD/Akt axis. *Cell Death Dis.* 2020;11(6):472.
- Soares-Lima SC, Mehanna H, Camuzi D, de Souza-Santos PT, Simão TA, Nicolau-Neto P, Almeida Lopes MS, Cuenin C, Talukdar FR, Batis N, Costa I, et al. Upper aerodigestive tract squamous cell carcinomas show distinct overall DNA methylation profiles and different molecular mechanisms behind WNT signaling disruption. *Cancers.* 2021;13(12):3014.
- Forrest ME, Khalil AM. Review: regulation of the cancer epigenome by long noncoding RNAs. *Cancer Lett.* 2017;407:106–12.

12. Yang W, Zhang K, Li L, Xu Y, Ma K, Xie H, Zhou J, Cai L, Gong Y, Gong K. Downregulation of lncRNA ZNF582-AS1 due to DNA hypermethylation promotes clear cell renal cell carcinoma growth and metastasis by regulating the N(6)-methyladenosine modification of MT-RNR1. *J Exp Clin Cancer Res.* 2021;40(1):92.
13. Wang B, Zhao L, Chi W, Cao H, Cui W, Meng W. Aberrant methylation-mediated downregulation of lncRNA SSTR5-AS1 promotes progression and metastasis of laryngeal squamous cell carcinoma. *Epigenetics Chromatin.* 2019;12(1):35.
14. Rupaimoole R, Slack FJ. MicroRNA therapeutics: towards a new era for the management of cancer and other diseases. *Nat Rev Drug Discov.* 2017;16(3):203–22.
15. Zhang Z, Zhang J, Fan C, Tang Y, Deng L. KATZLGO: large-scale prediction of lncRNA functions by using the KATZ measure based on multiple networks. *IEEE/ACM Trans Comput Biol Bioinform.* 2019;16(2):407–16.
16. Wang X, Zhang R, Wu S, Shen L, Ke M, Ouyang Y, Lin M, Lyu Y, Sun B, Zheng Z, Yang J, et al. Super-enhancer lncRNA LINC00162 promotes progression of bladder cancer. *iScience.* 2020;23(12):101857.
17. Doris SM, Chuang J, Viktorovskaya O, Murawska M, Spatt D, Churchman LS, Winston F. Spt6 is required for the fidelity of promoter selection. *Mol Cell.* 2018;72(4):687–699.
18. Ouda R, Sarai N, Nehru V, Patel MC, Debrosse M, Bachu M, Chereji RV, Eriksson PR, Clark DJ, Ozato K. SPT6 interacts with NSD2 and facilitates interferon-induced transcription. *FEBS Lett.* 2018;592(10):1681–92.
19. Diao C, Guo P, Yang W, Sun Y, Liao Y, Yan Y, Zhao A, Cai X, Hao J, Hu S, Yu W, et al. SPT6 recruits SND1 to co-activate human telomerase reverse transcriptase to promote colon cancer progression. *Mol Oncol.* 2021;15(4):1180–1202.
20. Pu J, Wang J, Wei H, Lu T, Wu X, Wu Y, Shao Z, Luo C, Lu Y. lncRNA MAGI2-AS3 prevents the development of HCC via recruiting KDM1A and promoting H3K4me2 demethylation of the RACGAP1 promoter. *Mol Ther Nucleic Acids.* 2019;18:351–62.
21. Sui Y, Chi W, Feng L, Jiang J. lncRNA MAGI2-AS3 is down-regulated in non-small cell lung cancer and may be a sponge of miR-25. *BMC Pulm Med.* 2020;20(1):59.
22. Dudas J, Ladanyi A, Ingruber J, Steinbichler TB, Riechelmann H. Epithelial to mesenchymal transition: a mechanism that fuels cancer radio/chemoresistance. *Cells.* 2020;9(2):428.
23. Yang J, Weinberg RA. Epithelial-mesenchymal transition: at the crossroads of development and tumor metastasis. *Dev Cell.* 2008;14(6):818–29.
24. Brabletz T, Kalluri R, Nieto MA, Weinberg RA. EMT in cancer. *Nat Rev Cancer.* 2018;18(2):128–34.
25. Huang D, Zhang K, Zheng W, Zhang R, Chen J, Du N, Xia Y, Long Y, Gu Y, Xu J, Deng M. Long noncoding RNA SGO1-AS1 inactivates TGFβ signaling by facilitating TGFB1/2 mRNA decay and inhibits gastric carcinoma metastasis. *J Exp Clin Cancer Res.* 2021;40(1):342.
26. Di Ruscio A, Ebralidze AK, Benoukraf T, Amabile G, Goff LA, Terragni J, Figueroa ME, De Figueiredo Pontes LL, Alberich-Jorda M, Zhang P, Wu M, et al. DNMT1-interacting RNAs block gene-specific DNA methylation. *Nature.* 2013;503(7476):371–76.
27. Wang F, Kong L, Pu Y, Chao F, Zang C, Qin W, Zhao F, Cai S. Long Noncoding RNA DICER1-AS1 functions in methylation regulation on the multi-drug resistance of osteosarcoma cells via miR-34a-5p and GADD45A. *Front Oncol.* 2021;11:685881.
28. Pan Z, Zhong B, Ling X, Zhang H, Tan Q, Huang D, Chen J, Zhang H, Zheng D, Li H, Chen X, et al. The DNMT1-associated lncRNA UCA1 was upregulated in TK6 cells transformed by long-term exposure to hydroquinone and benzene-exposed workers via DNA hypomethylation. *J Biochem Mol Toxicol.* 2021;35(12): e22920.
29. Xie G, Huang Z, Liu Z, Lin Z, Ma L. NCPHLDA: a novel method for human lncRNA-disease association prediction based on network consistency projection. *Molecular Omics.* 2019;15(6):442–50.
30. Wang B, Mei C, Wang Y, Zhou Y, Cheng MT, Zheng CH, Wang L, Zhang J, Chen P, Xiong Y. Imbalance data processing strategy for protein interaction sites prediction. *IEEE/ACM Trans Comput Biol Bioinform.* 2021;18(3):985–94.
31. Jiang L, Chen Q, Bei M, Shao M, Xu J. Characterizing the tumor RBP-ncRNA circuits by integrating transcriptomics, interactomics and clinical data. *Comput Struct Biotechnol J.* 2021;19:5235–45.
32. Lin Y, Zhang J, Cai J, Liang R, Chen G, Qin G, Han X, Yuan C, Liu Z, Li Y, Zou D, et al. Systematic analysis of gene expression alteration and co-expression network of eukaryotic initiation factor 4A-3 in cancer. *J Cancer.* 2018;9(24):4568–77.
33. Lu G, Chen L, Wu S, Feng Y, Lin T. Comprehensive analysis of tumor-infiltrating immune cells and relevant therapeutic strategy in esophageal cancer. *Dis Markers.* 2020;2020:8974793.